

# MPD Thruster Performance: Propellant Distribution and Species Effects

D. J. Merfeld,\* A. J. Kelly,† and R. G. Jahn‡  
*Princeton University, Princeton, New Jersey*

Previous research has shown that magnetoplasmadynamic thruster performance, as measured by thrust, specific impulse, and efficiency, is limited by a so-called "onset" current level. Experimental results show that the onset current level varies with the radial position of mass injection. Specifically, mass injection into either of two zones results in drastically different performance for both argon and xenon propellants. This difference in performance is evidenced by the onset current levels, the onset  $V$ - $J$  signatures, and the overall  $V$ - $J$  characteristics. The behavior of the thruster with the total mass flow split between the two zones follows a transition between the zonal behavioral limits. The behavior of propellant mixtures also follows a transition between the behavior of the individual propellant species. The flow region between the two zones is characterized by a particle number density discontinuity, a large axial current density, and a large electron Hall parameter, suggesting a possible correlation between observed onset phenomena and a shear-flow discontinuity located in the region between the two zones.

## Introduction

THE performance of the magnetoplasmadynamic (MPD) thruster, as measured by thrust, specific impulse, and efficiency, increases with current<sup>1</sup> and maximum thruster performance is limited, in terms of longevity and operating stability considerations, to a so-called "onset" current level. Above "onset," increasingly severe electrode and insulator ablation and unsteady and rapidly rising arc voltage are observed. Since it is well known that the performance limiting "onset" condition is related to the total mass flow, systematic study of the influence of propellant mass injection distribution seems worthwhile. It is the purpose of this paper to describe this approach to study the "onset" phenomena.

For this study, a standard "benchmark" multimegawatt MPD thruster was modified to permit independent propellant injection at four distinct radial positions. The test arrangement, shown schematically in Fig. 1, was carefully calibrated and used to explore voltage/current behavior, particularly onset conditions, for a broad array of mass injection distributions. Particular attention was focused on characterizing the two distinct operating states for propellant injection interior or exterior to a well-defined radial position for both argon and xenon propellants. Well-defined transitions were observed as the proportion of mass flow injected into the two zones was systematically varied.

In addition, the behavior of propellant mixtures was investigated. From these results, it is surmised that the region demarcating the two zones is characterized by a particle number density discontinuity, a large axial current density, and a large electron Hall parameter. This discontinuity may be some form of shear-flow plasma discontinuity that helps to define the "onset" phenomena.

## Experimental Setup

The thruster used in this study is a modified "benchmark" thruster (Fig. 1). This axially symmetric thruster has a discharge chamber that is 5.0 cm deep and 12.7 cm in diameter, with a Pyrex sidewall, a baron nitride backplate, and a 1.9 cm diam tungsten cathode. The annular aluminum anode is 1.0 cm thick, 18.6 cm in diameter, and has an orifice 10.2 cm in diameter.

A modification of the basic benchmark propellant distribution system allows independent mass injection at each of four sites, which are denoted by the approximate radius of the injection site. The outer, intermediate, and "barrel" injection sites consist of 12 evenly spaced 3 mm diam holes at radii of approximately 4, 3, and 2 cm, respectively. (The precise orifice centerline radii are 3.80, 2.85, and 1.95, respectively.) The inner injection site is annular and is located at the base of the 0.95 cm diam cathode (subsequently referred to as the 1 cm injection position).

Spectroscopic studies were carried out using a three-prism Steinheil G.H. glass spectrograph, which has a linear dispersion of 5.4-40 Å/mm within the range of 4300-6000 Å. The achromatic 4.8 cm diam focusing lens, which has a focal length of 14.7 cm, provides a vertical image of 9 cm on both sides of the MPD thruster centerline at an axial location 4 cm downstream of the anode face.

There are a number of ways by which the onset limit may be specified. The method used to define onset in the series of experiments using argon as the propellant is the observed correlation between voltage hash (megahertz level oscillation) and thruster ablation. It has previously been shown<sup>2</sup> that the thruster ablation increases drastically when the peak-to-peak voltage hash becomes approximately 10% of the total voltage. Since this 10% rule is simple and demonstrates reasonable accuracy, it is the method most commonly used to define the onset condition.

Since no such correlation has been drawn between voltage hash and the onset condition for xenon propellant, the method used to define onset is the observation of ablation product lines in spectrograms of the discharge. A series of spectrograms taken at various current levels are compared (Fig. 2). In almost all cases, a current level is easily identified above which significant amounts of ablation products are observable and below which few ablation products are seen. This criterion is quantitatively similar to the 10% voltage

Presented as Paper 85-2072 at the AIAA/DGLR/JSASS 18th International Electric Propulsion Conference, Alexandria, VA, Sept. 30-Oct. 2, 1985; received Oct. 29, 1985; revision received April 20, 1986. Copyright © American Institute of Aeronautics and Astronautics, Inc., 1986. All rights reserved.

\*Graduate Student, Electric Propulsion Laboratory (presently with Massachusetts Institute of Technology, Cambridge).

†Senior Research Engineer, Electric Propulsion Laboratory. Member AIAA.

‡Dean, School of Engineering and Applied Science. Fellow AIAA.

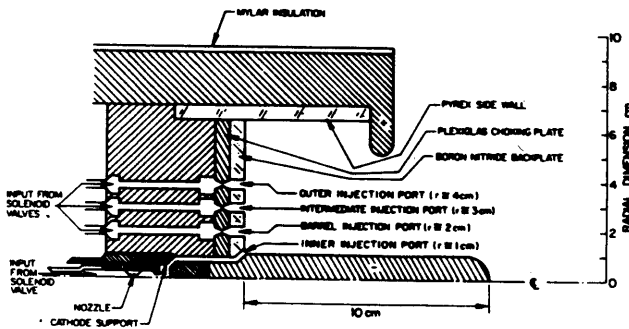


Fig. 1 Generalized propellant injection system benchmark thruster configuration.

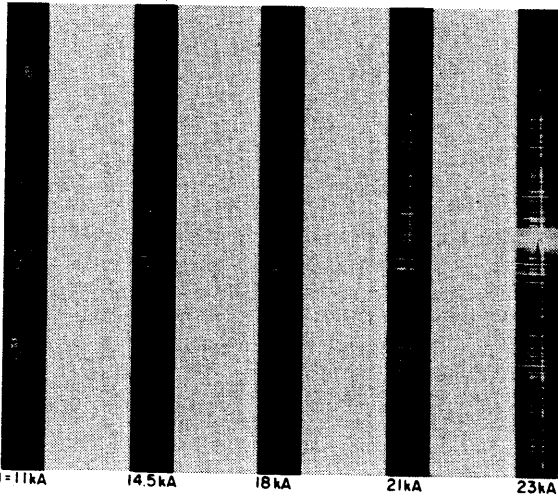


Fig. 2 Discharge spectra vs current ( $\dot{m} = 4$  g/s xenon,  $J^* = 19$  kA, 4 cm downstream of anode plane).

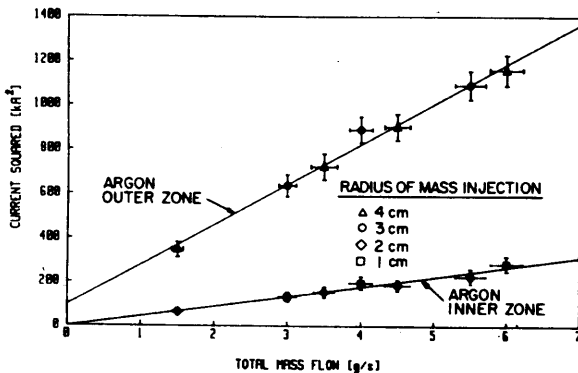


Fig. 3 Dependence of onset current on radius of mass injection (argon propellant).

hash criterion used for argon and helium, insofar as this measure of onset was established using the same spectroscopic basis.

### Zonal Definition

The dependence of the onset current on injection position was investigated by injecting argon or xenon propellant exclusively through each of the four injection sites. The onset current and a  $V$ - $J$  profile were then obtained for each injection site at several mass flow rates. The onset currents found using argon propellant indicate a distinct zonal behavioral pattern (Fig. 3). With equal propellant flow rates, the same onset current is obtained for injection at the 1 and 2 cm

sites. Injection at the 3 and 4 cm sites results in a substantially higher, but also well-defined onset current.

The importance of injection location is also emphasized by voltage/current signatures at current levels near onset (Figs. 4 and 5). For outer zone mass injection, the initial breakdown takes approximately  $300 \mu\text{s}$  to reach a quasisteady operating level; by comparison, inner zone mass injection results in breakdown transients on the order of  $200 \mu\text{s}$ . These transient durations are independent of the mass flow rate for all investigated values. However, while transient duration for the two inner zone injection sites is similar, the transient shape for the two cases is slightly different. This is best observed in Fig. 4, which shows that mass injection at the 1 cm site results in a more peaked hump on the voltage signal than that obtained for mass injection at the 2 cm site. Figure 5 displays a "humped" voltage trace without the usual steady region normally characteristic of quasisteady operation. While this behavior is not fully understood, it is considered not to be indicative of nonquasisteady operation.

Another clue to the zonal nature of the arc is provided by the  $V$ - $J$  characteristics. Figure 6 shows a plot of the nearly identical  $V$ - $J$  characteristics obtained for mass injection at the 3 and 4 cm sites. Figure 7 shows very similar  $V$ - $J$  characteristics for mass injection at the 1 and 2 cm sites. It is interesting to note that the inner zone  $V$ - $J$  characteristics fall directly on the outer zone characteristics until onset, indicating that the thruster behaves similarly, regardless of the injection pattern, until the inner zone onset limit is reached.

Since the inner zone is inside of a 3 cm radius, a transition region must fall somewhere between these radii, a region of the thruster that has been shown to exhibit very high Hall parameters and high axial current and electron densities for conditions above onset.<sup>2</sup>

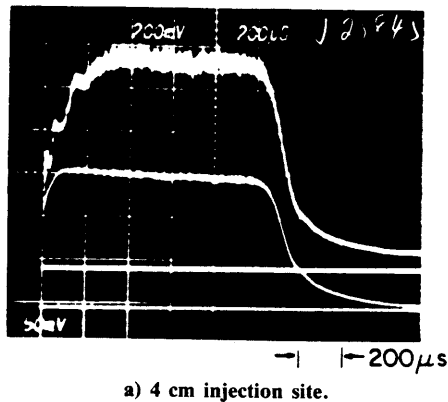
The measured onset currents indicate a zonal behavior for the xenon propellant that is similar to argon (Fig. 8). With equal propellant flow rate through either the 1 or 2 cm injection site, the same onset current is observed, whereas the 4 cm injection site results in another well-defined zonal limit. And once again, the onset current determined for the inner zone (1 and 2 cm sites) injection is substantially lower than that determined for the outer zone (4 cm site) injection.

One major difference between the xenon onset behavior and the argon onset behavior is shown in Fig. 9. With xenon propellant, the 3 cm data do not exhibit the zonal behavior observed for argon. In this case, the onset current initially determined for 3 cm injection is the same as that determined for the 4 cm site. However, as the mass flow is increased, the 3 cm onset current tends to fall toward the inner zone limit. This indicates that the zonal boundary is shifting such that at low mass flow rates the 3 cm site is part of the outer zone, while at higher mass flow rates the 3 cm site is part of the inner zone or, more likely, part of the transition region between the zones. Spectra also indicate that the transition region occurs near the 3 cm injection site. Many of the xenon ion spectral lines show a drop in intensity at a radius of approximately 3 cm (see Fig. 10).

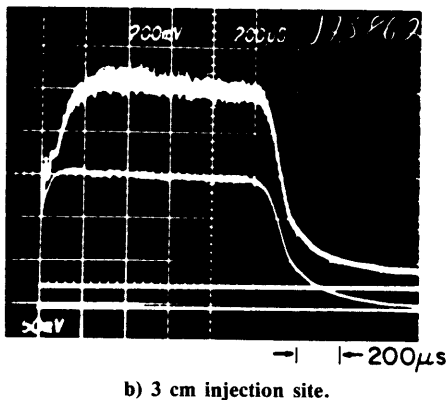
The cause of this intensity drop can be determined by looking at the variation of intensity with respect to number density and temperature. The intensity of any particular line is dependent on the particular geometry, the number density of the radiating species, and the Einstein coefficient of the particular line. If we assume that ion energy level populations can be adequately described by some ion temperature (i.e., possess a Boltzmann distribution)  $T_i$ , then the ratio of intensities of two ion lines, independent of number density, can be represented by

$$\frac{I_1}{I_2} = \frac{k_1}{k_2} e^{(E_2 - E_1)/kT_i} \quad (1)$$

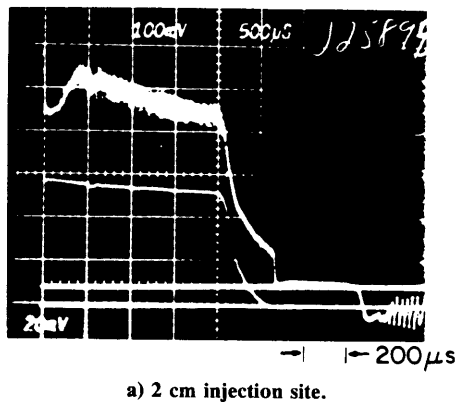
where  $I_1$  and  $I_2$  are the line intensities,  $E_1$  and  $E_2$  the ion upper level energies of the transitions,  $k_1$  and  $k_2$  constants for



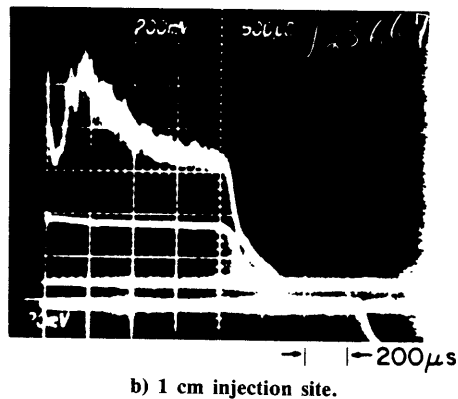
a) 4 cm injection site.



b) 3 cm injection site.



a) 2 cm injection site.



b) 1 cm injection site.

Fig. 4 Outer zone onset signatures (arc voltage, 50 V/div; arc current, 8.4 kA/div).

Fig. 5 Inner zone onset signatures (arc voltage, 20 V/div; arc current, 4.2 kA/div).

any two lines, and  $k$  Boltzmann's constant. Since the ratio of line intensities is nearly the same on either side of the discontinuity and over the entire length of the lines, we can deduce from Eq. (1) that the ion temperature is fairly uniform throughout the discharge chamber. Therefore, the observed intensity drop at the 3 cm position must be due to a drop in the ion number density as first suggested by Rudolph.<sup>2</sup>

This observed number density discontinuity and the peculiar behavior exhibited by the onset current for xenon injection at the 3 cm position suggest that the inner and outer zones are associated with the region of high and low number density respectively. This conclusion is also particularly true for nonequilibrium plasma in which the electron and ion temperatures differ. In these plasmas, the radiation is controlled by electron temperature which is known to be radially uniform.

**Zone Transitions**

Previous studies have shown that backplate ablation occurs near the cathode before the onset condition if inner zone mass injection is not present.<sup>3</sup> To slow this ablation, at least some mass should be injected in the inner zone. Thus, an optimization problem presents itself: enough inner zone mass should be injected to slow the inner zone ablation, yet outer zone flow is needed to maximize the onset current.

A series of experiments was conducted to investigate the manner in which onset current varies with mass injection distribution. These experiments were performed by beginning with a base mass flow level through one of the injection sites. Variable increments of mass flow were then added at one or the other injection sites and the onset current was determined for each of the experimental conditions.

The first transition curve (Fig. 11) was obtained by starting with a base mass flow of 3 g/s of argon through the 4 cm position. When increments of argon propellant were added at the 2 cm position, the onset current initially in-

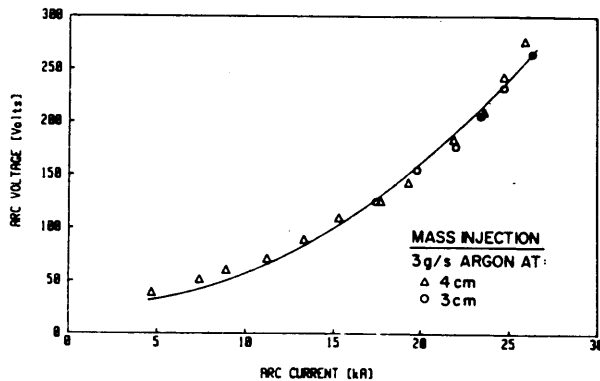


Fig. 6 Outer zone V-J characteristic (argon propellant).

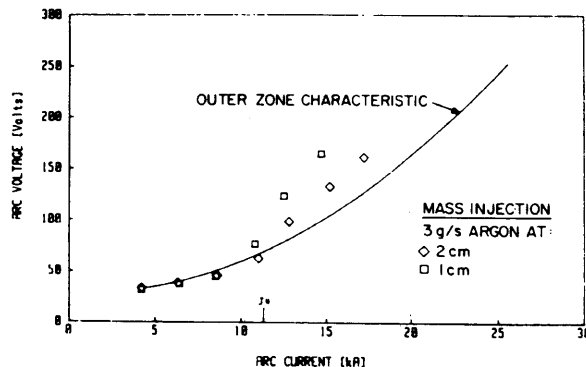


Fig. 7 Inner zone V-J characteristic (argon propellant).

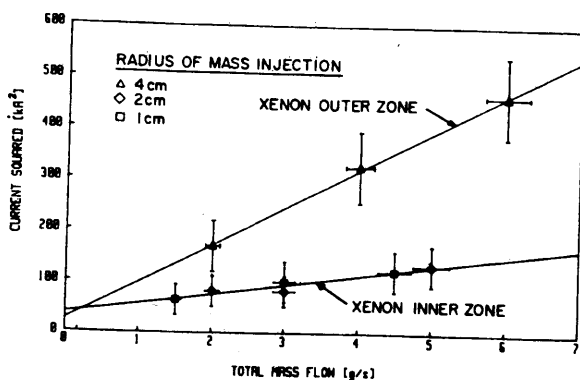


Fig. 8 Dependence of onset current on radius of mass injection (xenon propellant).

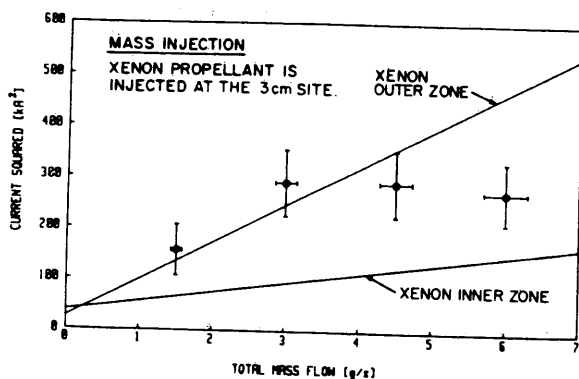


Fig. 9 Onset current for 3 cm injection site (xenon propellant).

creased as if the additional mass were being added through an outer zone injection site. This upward trend in the onset current ended quickly and eventually the onset current lowered to the point that it asymptotically approached the inner zone onset limit.

A second transition curve, shown on the same plot, was obtained with a base mass flow of 1.5 g/s through the 4 cm position. In this case, the same characteristic shape is seen indicating that a family of similarly shaped transition curves exist for the many possible base mass flow rates.

Another transition curve (Fig. 12) was obtained by beginning with a base mass flow of 3 g/s of argon at the 4 cm site and adding increments of argon propellant at the 1 cm site. Again, the curve asymptotically approaches the inner zone limit when the inner zone flow rate reaches approximately 3 g/s. However, the shape of the transition is somewhat different, having a somewhat oscillatory form.

A transition curve complementary to those previously described (Fig. 13) was obtained by beginning with a base argon flow of 1.5 g/s at the 2 cm site and by adding increments of argon propellant at the 4 cm site. Here, the transition started at the inner zone injection limit and slowly climbed to the outer zone injection limit. Compared to the outer-to-inner transitions, these transitions occurred very slowly, requiring a large ratio of outer mass flow to inner mass flow before approaching the outer zone limit. The relative abruptness of the outer-to-inner transitions indicates that the inner zone is a critical region in determining the limiting onset current, since only small amounts of mass flow within this region result in significantly decreased performance.

Xenon propellant test data exhibited the same basic transition behavior as observed with argon. When 1.5 g/s of xenon was injected at the 4 cm position and increments of xenon mass flow were injected at the 1 cm position, a very

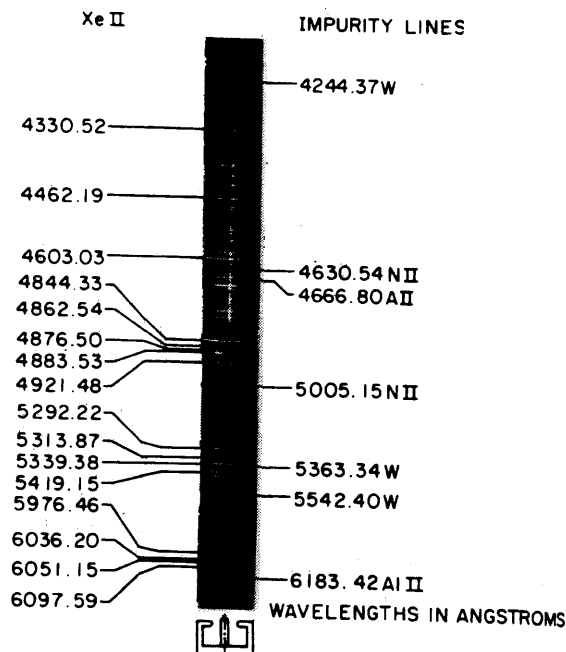


Fig. 10 Discharge spectra (xenon propellant),  $J = 21$  kA,  $m = 4$  g/s.

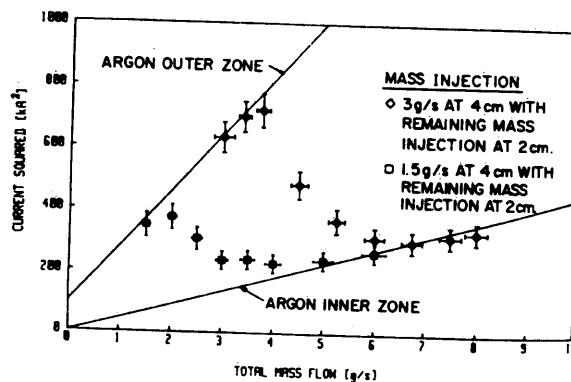


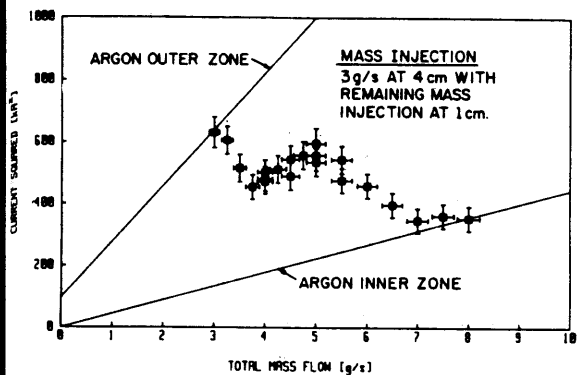
Fig. 11 Effect of argon injection at 2 cm on onset current (argon propellant).

gradual transition to the xenon inner zone limit was observed. (See Fig. 14.)

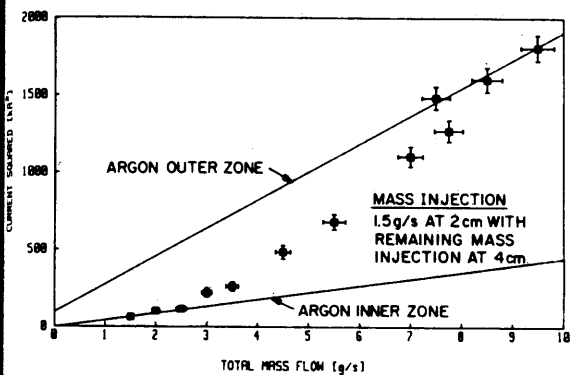
### Propellant Mixtures

Previous work<sup>4</sup> has shown that the addition of small amounts of helium to an argon arc results in large increases in the onset current. Further investigation of this effect was undertaken to understand the onset condition and to improve performance. A series of experiments was performed using a base mass flow of 3 g/s of argon through the 4 cm site. Small increments of helium or xenon were added through one of the other injection sites and the onset current was determined. It was found that if the base mass flow is added at the 4 cm site and helium is added at either inner zone injection site, a sharp increase in the onset limit occurs. (See Fig. 15.) On the other hand, if xenon is used as the auxiliary propellant, a slight decrease in the onset limit is evident for either inner zone injection site (Fig. 15). Nearly identical results are obtained when the auxiliary xenon and helium are added at the 3 cm site (Fig. 16).

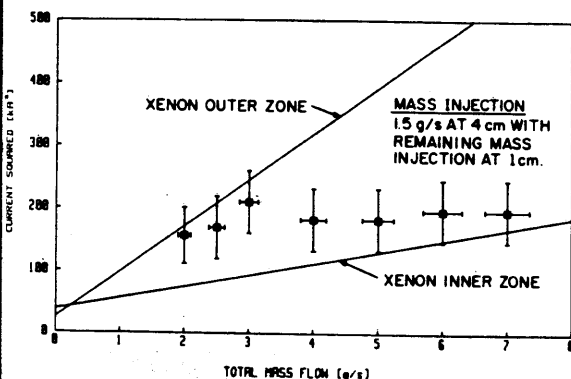
Previous investigators<sup>5</sup> have claimed that the onset parameter ( $J^2/m$ ) varies inversely with the square root of the molecular weight. In this view, the low molecular weight of helium causes the onset limit to be above those for argon and the xenon onset limit has already been shown to be



12 Effect of argon injection at 1 cm on onset current (argon propellant).



13 Effect of argon injection at 4 cm on onset current (argon propellant).



14 Effect of xenon injection at 1 cm on onset current (argon propellant).

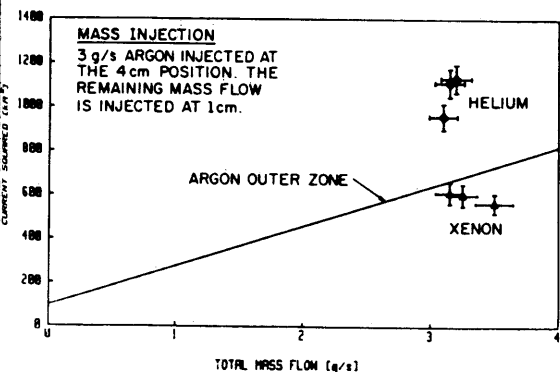


Fig. 15 Effect of mass injection at 1 cm on onset current.

below that of argon (Figs. 3 and 8). The experimental trends found here are thus consistent with this model.

To investigate further how onset behavior responds to propellant mixture change and to test the hypothesis that the auxiliary propellant data show the beginnings of transition curves, a base mass flow rate of 1.5 g/s of argon through the 4 cm position was augmented by increments of xenon propellant injected at the 1 cm position. In this case, Fig. 17 shows that a definite transition occurs from the argon outer zone limit to the xenon inner zone limit. This transition occurs between these limits in much the same manner as was observed for outer zone to inner zone transitions for both argon and xenon propellants. The complete transition exhibited by Fig. 17 is merely an extension of the partial transition of Fig. 15 (with a different base mass flow rate). Therefore, the hypothesis that Figs. 15 and 16 show the beginning of transition curves between propellant behavioral limits seems substantiated for the case of xenon auxiliary propellant. It is therefore probable that helium auxiliary propellant behavior also exhibits a transition between propellant limits.

One implication of these results is that it may be possible to tailor performance by propellant mixture, rather than being forced to employ unattractive pure propellants. For example, injection of small amounts of a propellant having a high  $J^{*2}/\dot{m}$  (such as helium) may improve onset performance.

### The Transition Zone

The physical details of the radial transition region have yet to be understood. In the interest of stimulating work on this matter and to provide a quantitative framework for an investigation into this phenomenon, it is suggested that the observed number density discontinuity is a shear-flow discontinuity of the type first described by Landau and Lifshitz<sup>6</sup> (cf, Sec. 53) and Appendix A of Merfeld.<sup>7</sup> The boundary conditions of such a discontinuity are

$$B_n = 0 \tag{2}$$

$$v_{t1} \neq v_{t2} \tag{3}$$

$$\rho_1 \neq \rho_2 \tag{4}$$

$$\rho_1 + B_{t1}^2/8\pi = \rho_2 + B_{t2}^2/8\pi \tag{5}$$

$$B_{t1} \neq B_{t2} \tag{6}$$

$$\dot{m}_n = 0 \tag{7}$$

where  $n$  and  $t$  are the directions normal and tangential to the discontinuity, 1 and 2 the two sides of the discontinuity,  $B$  the magnetic field,  $\rho$  the plasma density,  $v$  the plasma velocity,  $p$  the plasma pressure, and  $\dot{m}$  a mass flux.

In the MPD device, Eq. (2) is always satisfied due to the axisymmetric nature of the discharge. The tangential velocity discontinuity required by Eq. (3) has been observed by Boyle<sup>4</sup> for conditions above onset for a device similar to the present benchmark thruster. Also, the density discontinuity required by Eq. (4) has been observed and discussed by Rudolph.<sup>2</sup> Equations (5) and (6) are actually only one additional requirement. Since the ion and electron temperatures are nearly constant along radial profiles, the density discontinuity of Eq. (4) will result in a pressure discontinuity through a simple application of the ideal gas law. If a pressure discontinuity exists, then a magnetic field discontinuity is required to satisfy Eq. (5).

When the density is greater inside the discontinuity than outside, Eq. (5) requires that the magnetic field outside the discontinuity be greater than that inside. However, the intrusive nature of magnetic field probing precludes effective

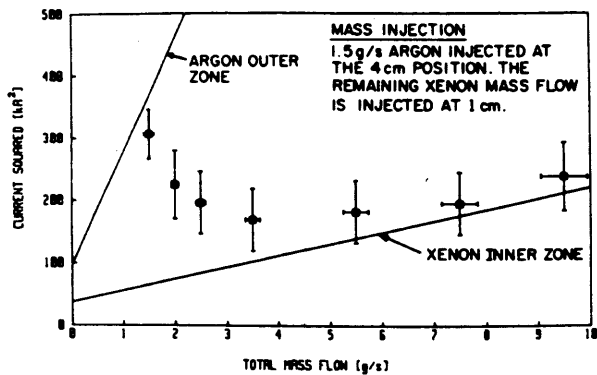


Fig. 16 Effect of mass injection at 3 cm on onset current.

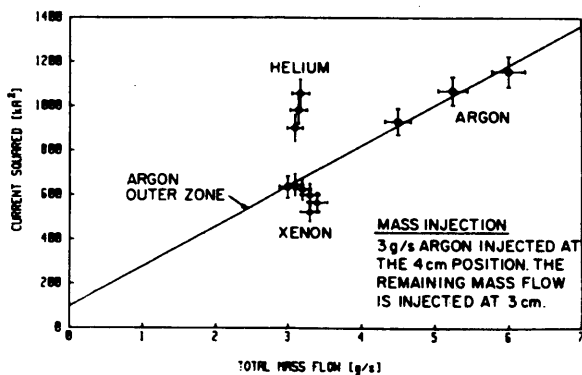


Fig. 17 Effect of xenon injection at 1 cm on onset current (xenon base propellant).

experimental verification. In addition, the general trend of the magnetic field amplitude is such that the field decreases in strength with increasing radius. This trend is opposite to the expected magnetic field jump across the discontinuity and the magnitude of the magnetic field trend is such that, unless measurements were taken just inside and outside of the discontinuity, the magnetic field jump could be masked by the overall trend. For these reasons, little experimental evidence can be offered to support a magnetic flux discontinuity at onset.

The final requirement [Eq. (7)] is that there be no mass flux normal to the discontinuity. Since radial plasma velocities are usually small in the MPD device, this condition is probably met.

Other experimental results also might be explained by the discontinuity idea. An example is the "stinger" effect

observed by Rudolph,<sup>2</sup> in which insertion of a quartz rod at a radius of between 1.5 and 2.5 cm inside of the discharge chamber results in large increases in the onset current. It is easy to imagine that the insertion of an ablating stinger into the vicinity of the discontinuity would alter the mass distribution and that the discontinuity position would delay onset condition to higher current levels.

The relative abruptness of the transition zone could also be explained by the idea of a discontinuity. Further work to determine order of magnitude estimates of the discontinuity thickness would be helpful in understanding the severity of this discontinuity.

### Summary and Conclusions

The principal conclusions from this study are:

- 1) A "zonal" behavior of discharge dependence on mass injection geometry is evident in onset current levels, onset  $V$ - $J$  signatures, and overall  $V$ - $J$  characteristics.
- 2) A number density discontinuity coincides with the position of the zonal transition region.
- 3) Transitions between zonal behaviors, as a function of propellant mass flow distribution, occur for both argon and xenon propellants.
- 4) Discharge behavior with propellant mixtures can be treated in terms of similar transitions.
- 5) A shear-flow discontinuity may be a possible cause of some onset phenomena.

### Acknowledgment

This work was supported by NASA/Jet Propulsion Laboratory Contract 954997.

### References

- <sup>1</sup>Jahn, R. G., *Physics of Electric Propulsion*, McGraw-Hill Book Co., New York, 1968.
- <sup>2</sup>Rudolph, L. K., "The MPD Thruster Onset Current Performance Limitation," Ph.D. Thesis, Mechanical and Applied Engineering Dept., Princeton University, Princeton, NJ, Sept. 1980.
- <sup>3</sup>Boyle, M. J., "Acceleration Processes in the Quasi-Steady Magnetoplasma Discharge," Ph.D. Thesis, Mechanical and Applied Engineering Dept., Princeton University, Princeton, NJ, Oct. 1974.
- <sup>4</sup>Boyle, M. J., "Pulsed Electromagnetic Gas Acceleration," Mechanical and Applied Engineering Dept., Princeton University, Princeton, NJ, MAE Rept. 1467h (JPL Contract 954997).
- <sup>5</sup>Hugel, H., "Effect of Self-Magnetic Forces on the Anode Mechanism of a High Current Discharge," *IEEE Transactions on Plasma Science*, Vol. PS-8, No. 4, Dec. 1980.
- <sup>6</sup>Landau, L. D. and Lifshitz, E. M., *Electrodynamics of Continuous Media*, Pergamon Press, Elmsford, NY, 1960.
- <sup>7</sup>Merfeld, D. M., "MPD Thruster Performance: Propellant Injection and Species Effects," M.S.E. Thesis, Mechanical and Applied Engineering Dept., Princeton University, Princeton, NJ, Oct. 1984.